

Imaging glial cell activation with [¹¹C]-R-PK11195 in patients with AIDS

Dima A Hammoud,¹ Christopher J Endres,¹ Ankit R Chander,¹ Tomas R Guilarte,² Dean F Wong,¹ Ned C Sacktor,³ Justin C McArthur,³ and Martin G Pomper¹

Departments of ¹Radiology and ³Neurology, the Johns Hopkins Medical Institutions; and Department of ²Environmental Health Sciences, Johns Hopkins School of Public Health, Baltimore, Maryland, USA

Glial cell activation occurs in response to brain injury and is present in a wide variety of inflammatory processes including dementia associated with human immunodeficiency virus (HIV). HIV-infected glial cells release cytokines and chemokines that, along with viral neurotoxins, contribute to neuronal damage and apoptosis. The purpose of this study was to determine if glial cell activation in HIV-positive (HIV+) patients could be detected noninvasively, *in vivo*, using [¹¹C]-R-PK11195 with positron emission tomography (PET). [¹¹C]-R-PK11195 is a selective radioligand for the peripheral benzodiazepine receptor (PBR), and is known to reflect the extent of glial cell activation. A subaim was to determine if nondemented HIV+ patients could be distinguished from those with HIV-associated dementia (HAD) on the basis of [¹¹C]-R-PK11195 binding. Five healthy volunteers and 10 HIV+ patients underwent PET with [¹¹C]-R-PK11195. Time-radioactivity curves (TACs) were generated from dynamic PET images in nine regions of interest (ROIs) drawn on coregistered magnetic resonance imaging (MRI) scans. The average radioactivity was calculated in each ROI and was normalized to the average radioactivity in white matter. Patients with HAD showed significantly higher [¹¹C]-R-PK11195 binding than controls in five out of eight brain regions ($P < .05$, Mann-Whitney *U* test). Nondemented HIV+ patients did not show significantly increased binding compared to controls. HIV+ patients overall (demented and nondemented) showed significantly higher radioligand binding than controls in five brain regions ($P < 0.05$). Patients with HAD did not show significant differences in binding when compared to HIV+ nondemented patients. The findings of this pilot study support a role for glial cell activation in HAD, and that PET with [¹¹C]-R-PK11195 can detect the concomitants of neuronal damage in individuals infected with HIV. *Journal of NeuroVirology* (2005) 11, 346–355.

Keywords: AIDS; HIV dementia; peripheral benzodiazepine receptor; PET; PK11195

Introduction

Central nervous system (CNS) infection with human immunodeficiency virus (HIV) is associated with the development of neurocognitive decline involving motor function (e.g., slowed movements, abnor-

mal gait, hypertonia), behavior (e.g., apathy, irritability, emotional lability), and cognition (e.g., attention, concentration, memory, information processing, language). In that context, a more severe form of neurocognitive decline is referred to as HIV-associated dementia (HAD), whereas the milder form is designated minor cognitive motor disorder or MCMD. The primary difference between the two is the degree of impairment in daily function. Whereas all but the most demanding aspects of daily function are spared in MCMD, there is a greater degree of impairment in HAD (American Academy of Neurology AIDS Task Force, 1991). Over the last few decades, although the incidence of HAD has fallen, the cumulative prevalence has actually risen (McArthur

Address correspondence to Martin G. Pomper, MD, PhD, Department of Radiology, Johns Hopkins University, 600 N. Wolfe Street, Phipps B-100, Baltimore, MD 21287-2182, USA. E-mail: mpomper@jhmi.edu

This work is supported by MH61438, the Johns Hopkins Center for AIDS Research (both to M.G.P.) and ES07062 (to T.R.G.).

Received 14 January 2005; revised 2 April 2005; accepted 12 May 2005.

et al, 2003). HAD currently constitutes about 5% of new acquired immunodeficiency syndrome (AIDS)-defining illnesses in the U.S. That may be due in part to the rising age of HIV+ individuals, with approximately 11% of HIV+ patients currently being 50 years of age or older, as well as to the influence of highly active antiretroviral therapy (HAART), which is nearly universally prescribed (McArthur *et al*, 2003).

Neurons are not believed to be infected actively by HIV (Kaul and Lipton, 2004; Kaul *et al*, 2001). It is currently believed that the majority of neurological damage in HAD is the result of glial cell activation by HIV-infected monocytes (Garden, 2002; McArthur *et al*, 2003; Gartner and Liu, 2002; Kaul *et al*, 2001), inducing the release of viral neurotoxins as well as a multitude of cytokines and chemokines, which contribute to neuronal damage and apoptosis (Lipton, 1993; Ilyin and Plata-Salaman, 1997; Kort, 1998; Chen *et al*, 1997; Conant *et al*, 1996). Examples of those viral proteins include, but are not limited to, Gp120 (envelope protein), Gp41, and Tat. Each of those proteins is known to cause indirect neuronal damage and induce apoptosis through the production and/or activation of different neurotoxic compounds including tumor necrosis factor (TNF)- α , interleukin (IL)-1, arachidonic acid metabolites of the cyclooxygenase and lipoxygenase pathways (Ilyin and Plata-Salaman, 1997), nuclear factor- κ B (Nicolini *et al*, 2001), monocyte chemoattractant protein (MCP)-1, platelet activating factor (PAF) (Gelbard *et al*, 1994; Jaranowska *et al*, 1995), a variety of excitatory amino acids (Brew *et al*, 1995; Gelbard *et al*, 1994; Yeh *et al*, 2000), free radicals, and nitric oxide.

Our purpose in this study was to determine if glial cell activation in HIV+ patients could be detected noninvasively, *in vivo*, using [11 C]-**R**-PK11195 (1-[2-chlorophenyl]-*N*-[11 C]methyl-*N*-[1-methyl-propyl]-3-isoquinolone carboxamide) with positron emission tomography (PET). PK11195 is an isoquinoline that binds selectively to the peripheral benzodiazepine receptor (PBR) in activated glial cells. [11 C]-**R**-PK11195 has been used as a noninvasive probe for imaging brain inflammation in a variety of disorders including multiple sclerosis (Vowinckel *et al*, 1997; Debruyne *et al*, 2002, 2003), stroke (Pappata *et al*, 2000), Rasmussen encephalitis (Banati *et al*, 1999), herpes encephalitis (Cagnin *et al*, 2001b), Alzheimer disease (Groom *et al*, 1995; Cagnin *et al*, 2001a), and amyotrophic lateral sclerosis (Turner *et al*, 2004). Recently [11 C]-**R**-PK11195 has been used to image nonhuman primate models of HIV (Venneti *et al*, 2004; Mankowski *et al*, 2003). [11 C]-**R**-PK11195 has a number of kinetic properties that permit its use as a marker for PBR *in vivo*: the extraction of [11 C]-**R**-PK11195 from blood to brain is rapid and high (>90%) and is unimpeded by the blood-brain barrier (BBB); i.e., tracer delivery is similar in areas with and without a BBB (Price *et al*, 1990; Banati, 2002).

The PBR is a multimeric complex localized to the outer mitochondrial membrane of the cell. PBR

is particularly abundant in peripheral organs and hematogenous cells, but is present in the normal CNS only at very low levels (Banati, 2002). The cellular and subcellular localization of PBR binding has been investigated in multiple models of neuronal injury, including ischemia, epilepsy, dementia, and demyelination, with occasionally conflicting results. Earlier studies showed that the distribution pattern of increased PBR expression more closely matched the distribution of activated microglia than that of reactive astrocytes (Banati *et al*, 1997; Myers *et al*, 1991; Stephenson *et al*, 1995; Benavides *et al*, 1991). More recent studies have shown that in addition to microglial activation there is also astrocytic activation correlated with PBR expression in the brain after injury. That was demonstrated in animal models (Kuhlmann and Guilarte, 1999; Chen *et al*, 2004) as well as in a human model of hippocampal sclerosis (Sauvageau *et al*, 2002). The reason for the discrepancy is probably because the earlier studies were focused on detecting changes acutely after injury with no long-term follow up, i.e., that there may be a temporal constraint dictating which subpopulation of glia is activated. Two recent studies describe a specific, temporal evolution of glial cell activation after injury, with earlier microglial activation followed by delayed astrocytic activation (Chen *et al*, 2004; Kuhlmann and Guilarte, 2000). The strength of the latter studies resides in the colocalization technique used, i.e., the ability to perform high-resolution [3 H]-**R**-PK11195 emulsion autoradiography concurrently with astrocyte immunostaining Glial fibrillary acidic protein (GFAP) and microglial immunostaining (MAC-1 or GSI-B4). That technique demonstrated clear colocalization of PBR expression to both microglia and astrocytes (Chen *et al*, 2004; Kuhlmann and Guilarte, 2000). Taken together, these data indicate that [11 C]-**R**-PK11195 (PBR expression) is a marker for the activation of glial cells in the CNS, with microglial and astrocytic contributions having different temporal profiles.

Results

Simulations

Across five subjects, the average fitted K_1 value in white matter (0.032 ml/min/ml) was only 23% of the value averaged across other brain regions (0.171 ml/min/ml), indicating very low relative blood flow in white matter. The average fitted k_3/k_4 values for the three subjects with HIV were roughly double the values of the two control subjects (Table 1). For each subject, the white matter k_3/k_4 value was comparable to those in cortical regions, indicating that the low activity in white matter did not reflect the absence of glial cell activation, and was mainly due to very low blood flow.

Simulation of white matter TACs used the following values: $K_1 = 0.032$ ml/min/ml, $K_1/k_2 = 0.2$ ml/min, $k_3 = 0.2$ min $^{-1}$, and baselevel $k_3/k_4 = 2.11$.

Table 1 Average k_3/k_4 values in controls and HIV+ subjects

Region	WM matter	CAU	CER	FRO	OCC	PON	PUT	TEM	THA
Controls (n = 2)	2.11	1.49	2.03	1.81	1.95	3.02	1.89	1.78	2.44
HIV (n = 3)	3.56	5.44	4.12	3.62	3.94	5.86	4.00	3.49	5.01

Note. Values are obtained from fitting regional TACs to a two-tissue, four-parameter blood input model, as described in the text. White matter (WM), caudate head (CAU), cerebellum (CER), frontal cortex (FRO), occipital cortex (OCC), pons (PON), putamen (PUT), temporal cortex (TEM), and thalamus (THA).

To represent other regions, time-radioactivity curves (TACs) were simulated with $K_1 = 0.171$ ml/min/ml, $K_1/k_2 = 0.2$ ml/ml, $k_3 = 0.2$ min⁻¹, and four baselevel values of k_3/k_4 (1.8, 2.3, 2.8, 3.3). Simulations were evaluated assuming a uniform global percent increase in activation. Thus for a TAC simulated with a k_3/k_4 value of 10% above baselevel, the analysis was performed using the white matter TAC with k_3/k_4 10% above baselevel. Table 2 shows that the relative radioligand binding increases as the global level of glial cell activation increases. The simulation results indicate that an increase in regional [¹¹C]-**R**-PK11195 binding is measurable even if there is increased activation in the white matter region used to normalize the binding.

Imaging

Compared to controls, patients with HAD showed significantly higher [¹¹C]-**R**-PK11195 binding in the thalamus, putamen, frontal, temporal and occipital cortex ($P < .05$, Mann-Whitney *U* test) (Table 3). There were, however, no significant differences in [¹¹C]-**R**-PK11195 binding between patients with Memorial Sloan-Kettering (MSK)-1 ($n = 2$) and MSK-2 ($n = 3$). Also, there was no difference in binding between the five different regions in patients with HAD that showed statistically greater [¹¹C]-**R**-PK11195 binding in comparison to controls, as these had similar absolute levels of increased binding (0.14 to 0.22).

HIV+ patients without dementia showed slightly higher [¹¹C]-**R**-PK11195 binding than controls in all regions; however, the difference did not reach statistical significance. Compared to controls, HIV+ patients as a group (nondemented and HAD) showed significantly higher [¹¹C]-**R**-PK11195 binding in the thalamus, putamen, cerebellum, frontal cortex, and occip-

ital cortex ($P < .05$, Mann-Whitney *U* test) (Table 3). HIV nondemented patients were not different from those with HAD on the basis of [¹¹C]-**R**-PK11195 binding (Table 3).

Discussion

We began this study by performing simulations to model PBR binding by [¹¹C]-**R**-PK11195 in search of a straightforward method by which to analyze our imaging data. Because glial cells are located throughout the brain, there is no true reference region for PK11195 binding. Given the absence of a true anatomic reference, a cluster analysis method has been described for extracting a reference TAC from the image data (Banati *et al*, 1999). That method assumes that in subjects with glial activation, a cluster TAC can be identified with similar kinetics to cortical TACs derived from normal subjects. It has been noted, however, that such a reference TAC cannot always be identified (Banati *et al*, 2000). The method of white matter normalization used here is based on the vastly reduced blood flow in white matter relative to other brain regions, as demonstrated in our modeling results. That low blood flow does not necessarily indicate low glial activation. In fact, due to slower radiotracer delivery, the white matter TAC integral is much less affected by glial activation than are the TAC integrals in other brain regions. Consequently, with white matter normalization, regional increases in [¹¹C]-**R**-PK11195 binding can be detected even when there is similar glial activation in white matter, as demonstrated by the simulation results (Table 2). Although, in theory, this method precludes measurement of [¹¹C]-**R**-PK11195 binding in the white matter itself, the simulations indicate that white matter

Table 2 [¹¹C]-**R**-PK11195 binding normalized to white matter

% k_3/k_4 above base level	0	10	20	40	60	80	100
Base level $k_3/k_4 = 1.8$	0.91	0.94	0.96	1.01	1.06	1.10	1.14
Base level $k_3/k_4 = 2.3$	1.09	1.12	1.14	1.19	1.24	1.28	1.31
Base level $k_3/k_4 = 2.8$	1.24	1.27	1.30	1.35	1.39	1.43	1.46
Base level $k_3/k_4 = 3.3$	1.38	1.41	1.44	1.48	1.52	1.55	1.57

Note. The relative binding was measured in simulated curves using white matter normalization as described in Materials and Methods. The baselevel binding values (k_3/k_4) cover the range of control binding levels (Table 1). The % increase in binding reflects different simulated levels of glial cell activation (PBR binding sites).

Table 3 Mean [¹¹C]-*R*-PK11195 binding measured in cortical and subcortical regions

ROI	Healthy controls (n = 5)	HIV+ patients/ nondemented (n = 5)	HIV+ patients/ HAD (n = 5)	HIV+ patients (HAD and nondemented) (n = 10)
Thalamus	1.60 (0.14)	1.76 (0.20)	1.81 (0.15)*	1.78 (0.17)*
Frontal	1.17 (0.07)	1.32 (0.17)	1.39 (0.15)*	1.36 (0.15)*
Temporal	1.22 (0.06)	1.33 (0.20)	1.39 (0.15)*	1.36 (0.17)
Occipital	1.28 (0.06)	1.54 (0.35)	1.47 (0.10)*	1.50 (0.25)*
Putamen	1.32 (0.08)	1.49 (0.19)	1.59 (0.09)*	1.54 (0.15)*
Caudate	1.15 (0.10)	1.25 (0.17)	1.21 (0.24)	1.23 (0.20)
Cerebellum	1.32 (0.05)	1.39 (0.06)	1.45 (0.13)	1.42 (0.10)*
Pons	1.68 (0.14)	1.84 (0.23)	1.72 (0.15)	1.78 (0.20)

Note. The values represent the mean regional activity averaged from 10 to 60 min postinjection, normalized to the mean activity in white matter. Standard deviations are shown in parentheses.

*Significantly different from control ($P < .05$, Mann-Whitney U test).

normalization enables measurement of increased uptake in gray matter regions.

We found significant differences in [¹¹C]-*R*-PK11195 binding between demented HIV+ patients and healthy controls in multiple regions of the brain, namely the thalamus, putamen, frontal cortex, temporal cortex, and occipital cortex. That is suggestive of brain glial cell activation in HAD, which is probably due to a higher number of glial cells as well as an increase in the binding sites per cell (Banati, 2002; Banati *et al*, 2000; Price *et al*, 1990). That finding is in keeping with the idea that microglial activation is believed to be responsible for the cascade of neuronal injury mediated by multiple viral proteins and other neurotoxic substances (Garden, 2002; McArthur *et al*, 2003; Gartner and Liu, 2002; Kaul *et al*, 2001; Lipton, 1993; Ilyin and Plata-Salaman, 1997; Kort, 1998; Chen *et al*, 1997; Conant *et al*, 1996). There was, however, no significant difference in tissue ratios between demented and nondemented HIV+ patients, or between controls and nondemented HIV+ patients.

Our results concur with the findings of two earlier studies that evaluated glial activation in animal models of HIV encephalitis using simian immunodeficiency virus (SIV) infected macaques (Mankowski *et al*, 2003; Venneti *et al*, 2004). In both studies, SIV-infected macaques that developed encephalitis (SIVE) demonstrated elevated levels of [³H]-*R*-PK11195 binding in frontal cortex (Mankowski *et al*, 2003) and in frontalwhite and gray matter, basal ganglia, and hippocampal areas (Venneti *et al*, 2004). In contrast, in an SIV-infected macaque without encephalitis, [³H]-*R*-PK11195 binding to frontal cortex was not elevated over control animal values (Mankowski *et al*, 2003).

Our results are also in concordance with published neuropathologic studies evaluating the cellular localization of HIV in the human brain. Using polymerase chain reaction with *in situ* hybridization for the detection of HIV DNA, and immunocytochemistry to identify the HIV-expressing cells, Takahashi *et al* found that the majority of infected cells were

macrophages and microglia with a substantial minority of cells harboring HIV DNA identified as astrocytes. Neurons, oligodendrocytes, and endothelial cells were not found to be infected with HIV, even in cases with HAD (Takahashi *et al*, 1996). Similar results favoring microglia/macrophages as the cellular targets of HIV infection in the brain were reached in other studies (Kure *et al*, 1990; Rottman *et al*, 1997; Vallat *et al*, 1998; Ward *et al*, 1987; Wesselingh *et al*, 1997). As for the topographical localization to different regions of the human brain, the putamen and thalamus were found in one study to be involved in the majority of cases, independent from the stage of disease (Neuen-Jacob *et al*, 1993). This is in concordance with our finding of significant differences in [¹¹C]-*R*-PK11195 binding in patients with HAD and in HIV-infected patients (demented and nondemented) compared to controls in those two regions. Similarly, in another study, although there was no global quantitative correlation between cortical neuronal apoptosis and HIV encephalitis or microglial activation, there was still some topographical correlation between these changes (Adle-Biassette *et al*, 1999).

Three out of the 10 participating HIV+ subjects were not on antiretroviral (ARV) therapy at the time of the study, two of whom were demented. We do not know whether ARV therapy affected the results of the PET studies in those patients, as there were no significant differences in [¹¹C]-*R*-PK11195 binding between those patients and their corresponding groups. However, in view of our small sample size, it will be difficult to define with certainty the effect of ARV therapy on [¹¹C]-*R*-PK11195 binding.

Only one patient in this study (MSK-2) was undergoing treatment with benzodiazepines. However, we do not expect this to affect our measurements because the agent used, clonazepam, binds to the central benzodiazepine receptors and not to PBR.

Our results are also in concordance with findings on magnetic resonance (MR) spectroscopy (MRS) in HAD, as described in the literature. Several recent studies demonstrated altered metabolite levels

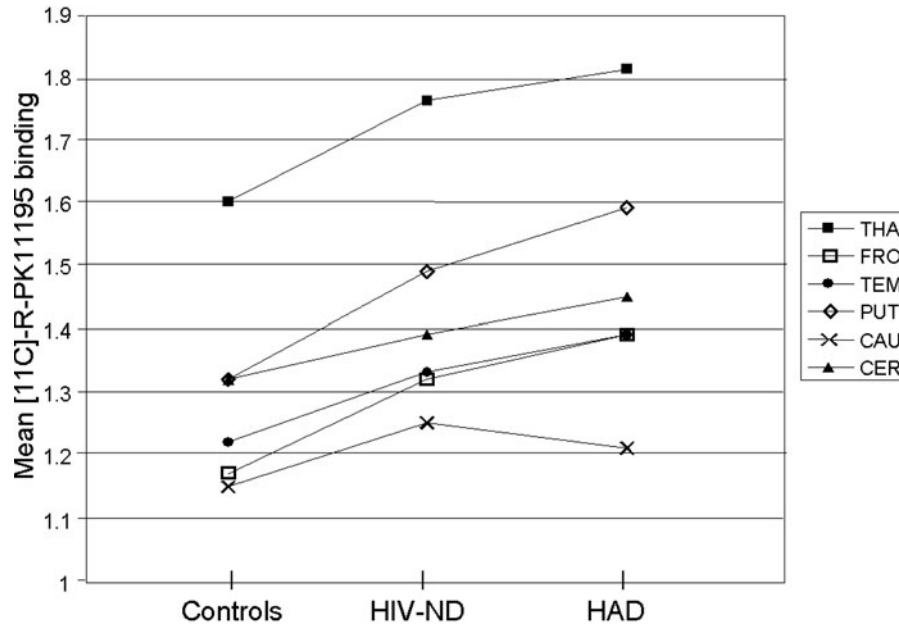


Figure 1 Scatter plot of the mean [^{11}C]-*R*-PK11195 binding in correlation to the three groups of subjects: controls, HIV+ nondemented (HIV-ND), and HIV+ demented [HAD] patients in different brain regions (thalamus [THA], frontal lobe [FRO], temporal lobe [TEM], putamen [PUT], caudate [CAU] and cerebellum [CER]).

in HIV patients with or without dementia (Chang *et al*, 2004; Ernst *et al*, 2003; von Giesen *et al*, 2001), namely increases of metabolites reflective of glial activation such as *myo*-inositol (MI) and choline (ChO) and decreases of markers of neuronal viability such as *N*-acetylaspartate (NAA). In one large multicenter *in vivo* MRS study, the authors concluded that their results suggest that glial activation occurs during the asymptomatic stage of HIV-infection, whereas further inflammatory activity in the basal ganglia and neuronal injury in the white matter is associated with the development of cognitive impairment (Chang *et al*, 2004). Similarly, in another study, HIV-demented patients exhibited higher Cho/Cr (creatinine) and MI/Cr in the basal ganglia, significantly reduced NAA/Cr, and significantly increased MI/Cr in the frontal white matter compared to controls (Lee *et al*, 2003).

Our findings suggest that although HIV infection of the CNS occurs soon after the initial infection, HAD occurs only later once significant neuronal injury has occurred. The delayed activation of the microglia and secondary neuronal injury are related both to the viral load and the immunological status of the patient. In fact, it was found that the brains of asymptomatic HIV+ individuals contain no, or very little, viral DNA (Donaldson *et al*, 1994; Bell *et al*, 1993). It is well known that as HIV/AIDS progresses, the proportion of circulating, activated monocytes increases (Pulliam *et al*, 1997; Gartner, 2000), leading to more trafficking of these cells into the CNS. The peripheral activation of circulating monocytes is probably a critical step that

permits their ingress to the brain (Gartner, 2000). Our findings support the theory that early in the disease, a limited infection occurs with some microglial activation but not enough neurotoxicity to produce symptoms. The lack of a difference in [^{11}C]-*R*-PK11195 binding between nondemented HIV+ patients and individuals with HAD is suggestive of a spectrum of pathology that starts around the time of infection and progresses slowly (Figure 1). It appears that reseeded of the CNS by activated monocytes later in the disease, after the development of immunosuppression, induces a productive CNS infection (Gartner and Liu, 2002), with secondary onset of neurological signs consistent with HAD. That pathophysiologic mechanism is further supported by the fact that the incidence of HAD has markedly decreased with the use of HAART. Because many antiretroviral medications do not penetrate the BBB (McArthur *et al*, 2003), the reduction of HAD incidence must be related in part to the peripheral effect of HAART on the viral load and state of immunosuppression.

By using [^{11}C]-*R*-PK11195, a selective PBR ligand believed to reflect glial cell activation in the brain, we were able to demonstrate a significant difference in binding between demented HIV+ patients and healthy controls as well as between HIV+ patients in general (with or without HAD) and healthy controls. That supports the theory advocating the role of glial cell activation in HAD. Both early and late activation of glial cells should be measurable with [^{11}C]-*R*-PK11195, as PBR overexpression is present at both times, although in different subsets of cells (Chen *et al*, 2004). However, this is a pilot study with

a limited number of patients. The small sample size likely accounts for the lack of significant differences between HIV+ nondemented and HAD patients and between HIV+ nondemented patients and controls. The small sample size also likely accounts for the lack of significant differences in some brain regions between patients with HAD and controls. However, we still detected trends of incremental increased uptake, with HAD patients having the highest uptake, followed by nondemented HIV+ patients followed by controls (see Figure 1). Therefore, we suspect that a larger study would enable differentiation between the three groups and assessment of the effect of ARV therapy on [¹¹C]-**R**-PK11195 binding and will likely validate further the usefulness of [11C]-**R**-PK11195 PET imaging in HAD for diagnosis and therapeutic monitoring.

Materials and methods

Human subjects

Fifteen subjects, including 5 healthy volunteers and 10 patients diagnosed with HIV (HIV+) were included in this study. All subjects were males except for one healthy female volunteer. Using full neuropsychological testing, the patients were stratified based on the Memorial Sloan-Kettering dementia (MSK) scale. The MSK scale is a commonly used method of HAD clinical staging, based on functional, intellectual, and motor impairment. The scores range from 0 (normal) to 4 (end stage). Five of the 10 HIV+ patients were diagnosed with dementia (2 patients with severity scale of 1 (MSK-1) and 3 patients with MSK-2). The three-patient subgroups were age-matched: healthy controls (41 ± 10 years), HIV nondemented (45 ± 8 years), HIV demented (HAD) (44 ± 6 years). There were no significant age differences between any subgroups ($P > .45$, two-tailed t test).

Three of the HIV+ subjects were not on ARV therapy at the time of the study, two of whom were demented. Only one demented patient was treated for assumed intracranial toxoplasmosis 6 months before the PET scan, with complete response to therapy and resolution of abnormal contrast enhancement on magnetic resonance imaging (MRI) by the time the PET study was performed. None of the other patients was documented to have an opportunistic infection over at least 2 years prior to the PET scan and none of them had any evidence of intracranial opportunistic infection at the time of the study.

The Johns Hopkins Joint Committee on Clinical Investigation approved the protocol, and all subjects provided signed, informed consent prior to entry into the study.

Simulations

Simulations of [¹¹C]-**R**-PK11195 kinetics were based on a two-tissue four-parameter (K_1 , k_2 , k_3 , k_4)

receptor-ligand model, plus a blood volume term (V_b) to account for vascular radioactivity. To derive appropriate parameter values, cerebral TACs for the five subjects (two controls, one HIV nondemented, two HIV with dementia) that had arterial blood sampling were fit to the receptor-ligand model. Based on previously reported parameter values (Kropholler *et al*, 2004), and assuming a constant plasma-to-blood ratio of 1.66, nonspecific binding (K_1/k_2) was set to 0.2 and blood volume was set to 0.04 ml/ml. The three remaining parameters (K_1 , k_3 , k_3/k_4) were determined from curve fitting. For simulations, an input function and total plasma curve from a control subject were used, along with mean fitted values of K_1 in white matter and other brain regions. It was assumed that controls had minimal glial cell activation, thus baselevel values of k_3/k_4 were selected to encompass the range of values measured in the two control subjects. To simulate glial activation, baselevel values of k_3/k_4 were increased by 10%, 20%, 40%, 60%, 80%, and 100%, which roughly covered the range of k_3/k_4 values measured in the three HIV+ subjects. The binding of [¹¹C]-**R**-PK11195 was measured from the simulated curves as described above, i.e., by integrating the curves from 10 to 60 min and normalizing to the white matter TAC integral. The effects of specific binding level (k_3/k_4) on the measured [¹¹C]-**R**-PK11195 binding are reported.

Image acquisition

A thermoplastic mask was fitted to each subject's face for the purpose of immobilization and positioning during scanning. For 12 of the 15 subjects, magnetic resonance images were acquired using a 1.5-T Signa Advantage system (GE Medical Systems, Milwaukee, WI, USA) and a three-dimensional (3D) SPGR (spoiled gradient recalled acquisition in the steady state) sequence with the following parameters: repetition time 50 ms, echo time 5 ms, flip angle of 45 degrees, number of excitations 1, field of view = 24 × 24 cm, slice thickness = 1.5 mm, and reconstruction matrix of 256 × 256, yielding an in-plane pixel size of 0.93 × 0.93 mm. For the PET studies, a 10-min transmission scan was obtained prior to radioligand administration. An intravenous bolus of 19.7 ± 1.4 mCi (17 to 22 mCi; 0.629 to 0.814 MBq) of [¹¹C]-**R**-PK11195 at high specific activity (>5000 Ci/mmol) was administered intravenously in a solution of 0.9% sodium chloride. PET data were acquired on a GE Advance scanner (General Electric, USA) in 3D mode, which acquires 35 simultaneous slices with an interslice separation of 4.25 mm (DeGrado *et al*, 1994). Twenty-four sets of scans were acquired over 60 min (4 × 15 s, 4 × 30 s, 3 × 60 s, 2 × 120 s, 5 × 240 s, 6 × 300 s). PET images were reconstructed using a ramp reconstruction filter and a 25.6 cm by 25.6 cm field of view into a 128 × 128 pixel matrix. The final resolution at full width half maximum (FWHM) with these parameters is 5 mm

in-plane. Images were decay corrected to the time of injection.

Blood sampling

Arterial blood samples were taken from five subjects (two controls, one HIV nondemented, two HIV with dementia) during PET scanning. Following bolus injection of [^{11}C]-*R*-PK11195, blood was sampled from a radial arterial catheter as fast as possible for the first 90 s, then at times of 2, 2.5, 3, 5, 10, 15, 20, 25, 30, 45, and 60 min post injection. The sampling volume was 1.0 ml, with larger samples (4 ml) taken at 3, 10, 20, 30, 45, and 60 min to provide additional blood for assay of radioactive metabolites. To measure total plasma radioactivity, whole blood samples were centrifuged, and 0.5 ml of plasma was counted for 1 min in a NaI well counter (CompuGamma CS by Wallac Oy, Turku, Finland). The assay for plasma radioactive metabolites employed a column switch high-performance liquid chromatography (HPLC) method (Hilton *et al*, 2000).

Data analysis

For 12 of the 15 subjects, MRI images were coregistered to a mean PET image using the mutual information algorithm in SPM2 (Wellcome Department of Cognitive Neurology, London, UK) in MATLAB (MathWorks, MA). For the three subjects who did not have MRI scans, the Montreal Neurological Institute (MNI) Atlas was applied to obtain an anatomical reference for region drawing. To create an appropriate template, the MRI scans of five subjects

were normalized to the MNI Atlas, and the normalization was applied to the corresponding mean PET images. The five normalized PET scans were then averaged and smoothed ($8 \times 8 \times 8$ cm) to generate a PET template in the same space as the MNI Atlas. For the three subjects who did not have MRI, their mean PET images were normalized to the PET template. The inverse normalization was then applied to the MNI Atlas, which effectively produced a substitute MRI scan in the same space as the original PET scan. Processing of regions-of-interest (ROIs) was performed using Analyze software (Mayo foundation, Rochester, MN) (Robb, 2001). ROIs were hand drawn on the coregistered MRI images, with three image slices used for each of the following structures: caudate head (CAU), putamen (PUT), thalamus (THA), frontal cortex (FRO), occipital cortex (OCC), temporal cortex (TEM), pons (PON), cerebellum (CER), and white matter (WM). The ROIs were then applied to the dynamic PET images to generate TACs. To evaluate [^{11}C]-*R*-PK11195 binding, the average activity (10 to 60 min) in gray matter regions was divided by the average activity in white matter (10 to 60 min). The white matter was used to normalize radiotracer binding because it showed the lowest overall activity (Figure 2), and provided a stable reference value; the mean coefficient of variation of the white matter TAC from 10 to 60 min was only 6.4%. Because white matter is not a true reference region for glial cell activation, simulations were applied to examine the effects of specific binding in white matter on the measured binding of [^{11}C]-*R*-PK11195.

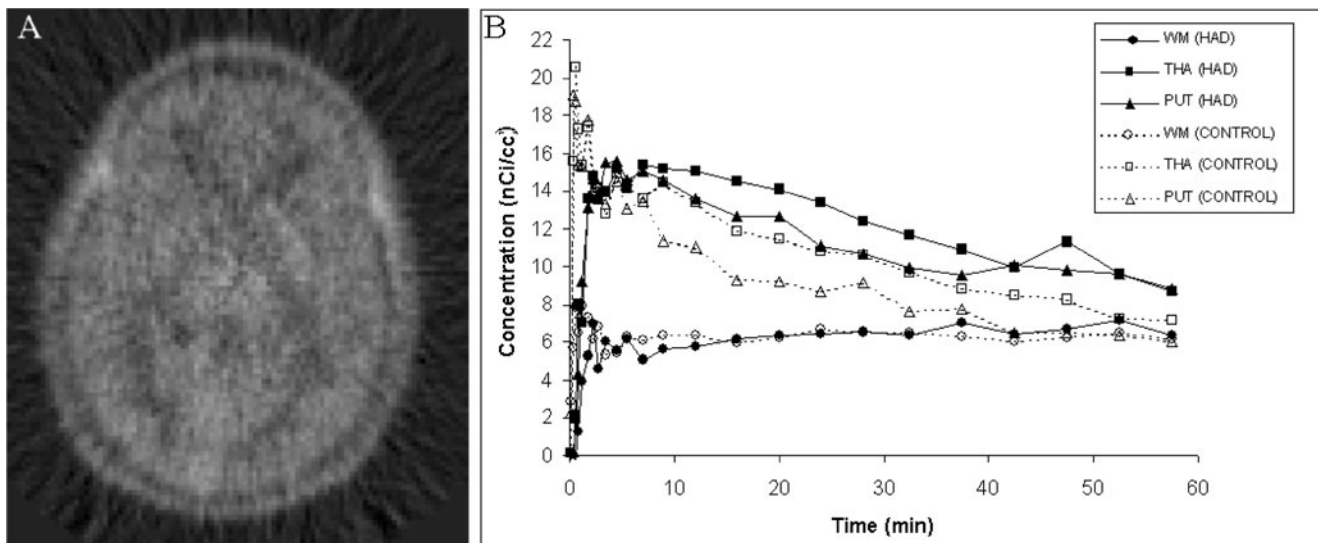


Figure 2 (A) PET image of a patient with HAD; (B) TACs from three different regions of the brain in a patient with HAD and control, normalized to the injected dose. Note that the white matter (WM) activity in both patients is similar with less binding and relatively stable clearance relative to the other ROIs. The putamen (PUT) and thalamus (THA) show slower clearance in the HAD patient, compared to the control.

References

- Ahle-Biassette H, Chretien F, Wingertsmann L, Hery C, Ereau T, Scaravilli F, Tardieu M, Gray F (1999). Neuronal apoptosis does not correlate with dementia in HIV infection but is related to microglial activation and axonal damage. *Neuropathol Appl Neurobiol* **25**: 123–133.
- American Academy of Neurology AIDS Task Force A (1991). Nomenclature and research case definitions for neurologic manifestations of human immunodeficiency virus-type 1 (HIV-1) infection. Report of a Working Group of the American Academy of Neurology AIDS Task Force. *Neurology* **41**: 778–785.
- Banati RB (2002). Visualising microglial activation in vivo. *Glia* **40**: 206–217.
- Banati RB, Goerres GW, Myers R, Gunn RN, Turkheimer FE, Kreutzberg GW, Brooks DJ, Jones T, Duncan JS (1999). [¹¹C](R)-PK11195 positron emission tomography imaging of activated microglia in vivo in Rasmussen's encephalitis. *Neurology* **53**: 2199–2203.
- Banati RB, Myers R, Kreutzberg GW (1997). PK ('peripheral benzodiazepine')-binding sites in the CNS indicate early and discrete brain lesions: microautoradiographic detection of [³H]PK11195 binding to activated microglia. *J Neurocytol* **26**: 77–82.
- Banati RB, Newcombe J, Gunn RN, Cagnin A, Turkheimer F, Heppner F, Price G, Wegner F, Giovannoni G, Miller DH, Perkin GD, Smith T, Hewson AK, Bydder G, Kreutzberg GW, Jones T, Cuzner ML, Myers R (2000). The peripheral benzodiazepine binding site in the brain in multiple sclerosis: quantitative in vivo imaging of microglia as a measure of disease activity. *Brain* **123**(Pt 11): 2321–2337.
- Bell JE, Busuttill A, Ironside JW, Rebus S, Donaldson YK, Simmonds P, Peutherer JF (1993). Human immunodeficiency virus and the brain: investigation of virus load and neuropathologic changes in pre-AIDS subjects. *J Infect Dis* **168**: 818–824.
- Benavides J, Bourdiol F, Dubois A, Scatton B (1991). Regional pattern of increased omega 3 (peripheral type benzodiazepine) binding site densities in the rat brain induced by systemic injection of kainic acid. *Neurosci Lett* **125**: 219–222.
- Brew BJ, Corbeil J, Pemberton L, Evans L, Saito K, Penny R, Cooper DA, Heyes MP (1995). Quinolinic acid production is related to macrophage tropic isolates of HIV-1. *J NeuroVirol* **1**: 369–374.
- Cagnin A, Brooks DJ, Kennedy AM, Gunn RN, Myers R, Turkheimer FE, Jones T, Banati RB (2001a). In-vivo measurement of activated microglia in dementia. *Lancet* **358**: 461–467.
- Cagnin A, Myers R, Gunn RN, Lawrence AD, Stevens T, Kreutzberg GW, Jones T, Banati RB (2001b). In vivo visualization of activated glia by [¹¹C] (R)-PK11195-PET following herpes encephalitis reveals projected neuronal damage beyond the primary focal lesion. *Brain* **124**: 2014–2027.
- Chang L, Lee PL, Yiannoutsos CT, Ernst T, Marra CM, Richards T, Kolson D, Schifitto G, Jarvik JG, Miller EN, Lenkinski R, Gonzalez G, Navia BA (2004). A multicenter in vivo proton-MRS study of HIV-associated dementia and its relationship to age. *Neuroimage* **23**: 1336–1347.
- Chen MK, Baidoo K, Verina T, Guilarte TR (2004). Peripheral benzodiazepine receptor imaging in CNS demyelination: functional implications of anatomical and cellular localization. *Brain* **127**: 1379–1392.
- Chen P, Mayne M, Power C, Nath A (1997). The Tat protein of HIV-1 induces tumor necrosis factor-alpha production. Implications for HIV-1-associated neurological diseases. *J Biol Chem* **272**: 22385–22388.
- Conant K, Ma M, Nath A, Major EO (1996). Extracellular human immunodeficiency virus type 1 Tat protein is associated with an increase in both NF-kappa B binding and protein kinase C activity in primary human astrocytes. *J Virol* **70**: 1384–1389.
- Debruyne JC, Van Laere KJ, Versijpt J, De Vos F, Eng JK, Strijckmans K, Santens P, Achten E, Slegers G, Korf J, Dierckx RA, De Reuck JL (2002). Semiquantification of the peripheral-type benzodiazepine ligand [¹¹C]PK11195 in normal human brain and application in multiple sclerosis patients. *Acta Neurol Belg* **102**: 127–135.
- Debruyne JC, Versijpt J, Van Laere KJ, De Vos F, Keppens J, Strijckmans K, Achten E, Slegers G, Dierckx RA, Korf J, De Reuck JL (2003). PET visualization of microglia in multiple sclerosis patients using [¹¹C]PK11195. *Eur J Neurol* **10**: 257–264.
- DeGrado TR, Turkington TG, Williams JJ, Stearns CW, Hoffman JM, Coleman RE (1994). Performance characteristics of a whole-body PET scanner. *J Nucl Med* **35**: 1398–1406.
- Donaldson YK, Bell JE, Ironside JW, Brettell RP, Robertson JR, Busuttill A, Simmonds P (1994). Redistribution of HIV outside the lymphoid system with onset of AIDS. *Lancet* **343**: 383–385.
- Ernst T, Chang L, Arnold S (2003). Increased glial metabolites predict increased working memory network activation in HIV brain injury. *Neuroimage* **19**: 1686–1693.
- Garden GA (2002). Microglia in human immunodeficiency virus-associated neurodegeneration. *Glia* **40**: 240–251.
- Gartner S (2000). HIV infection and dementia. *Science* **287**: 602–604.
- Gartner S, Liu Y (2002). Insights into the role of immune activation in HIV neuropathogenesis. *J NeuroVirol* **8**: 69–75.
- Gelbard HA, Nottet HS, Swindells S, Jett M, Dzenko KA, Genis P, White R, Wang L, Choi YB, Zhang D, et al. (1994). Platelet-activating factor: a candidate human immunodeficiency virus type 1-induced neurotoxin. *J Virol* **68**: 4628–4635.
- Groom GN, Junck L, Foster NL, Frey KA, Kuhl DE (1995). PET of peripheral benzodiazepine binding sites in the microgliosis of Alzheimer's disease. *J Nucl Med* **36**: 2207–2210.
- Hilton J, Yokoi F, Dannals RF, Ravert HT, Szabo Z, Wong DF (2000). Column-switching HPLC for the analysis of plasma in PET imaging studies. *Nucl Med Biol* **27**: 627–630.
- Ilyin SE, Plata-Salaman CR (1997). HIV-1 envelope glycoprotein 120 regulates brain IL-1beta system and TNF-alpha mRNAs in vivo. *Brain Res Bull* **44**: 67–73.
- Jaranowska A, Bussolino F, Sogos V, Arese M, Lauro GM, Gremo F (1995). Platelet-activating factor production by human fetal microglia. Effect of lipopolysaccharides and tumor necrosis factor-alpha. *Mol Chem Neuropathol* **24**: 95–106.

- Kaul M, Garden GA, Lipton SA (2001). Pathways to neuronal injury and apoptosis in HIV-associated dementia. *Nature* **410**: 988–994.
- Kaul M, Lipton SA (2004). Signaling pathways to neuronal damage and apoptosis in human immunodeficiency virus type 1-associated dementia: chemokine receptors, excitotoxicity, and beyond. *J NeuroVirol* **10**(Suppl 1): 97–101.
- Kort JJ (1998). Impairment of excitatory amino acid transport in astroglial cells infected with the human immunodeficiency virus type 1. *AIDS Res Hum Retroviruses* **14**: 1329–1339.
- Kropholler MA, Boellaard R, Schuitemaker A, Van Berckel B, Lammertsma AA (2004). Development of a plasma input model for analysis of [¹¹C](R)-PK11195 studies. *NeuroImage* **22**: T184–T185.
- Kuhlmann AC, Guilarte TR (1999). Regional and temporal expression of the peripheral benzodiazepine receptor in MPTP neurotoxicity. *Toxicol Sci* **48**: 107–116.
- Kuhlmann AC, Guilarte TR (2000). Cellular and subcellular localization of peripheral benzodiazepine receptors after trimethyltin neurotoxicity. *J Neurochem* **74**: 1694–1704.
- Kure K, Lyman WD, Weidenheim KM, Dickson DW (1990). Cellular localization of an HIV-1 antigen in subacute AIDS encephalitis using an improved double-labeling immunohistochemical method. *Am J Pathol* **136**: 1085–1092.
- Lee PL, Yiannoutsos CT, Ernst T, Chang L, Marra CM, Jarvik JG, Richards TL, Kwok EW, Kolson DL, Simpson D, Tang CY, Schifitto G, Ketonen LM, Meyerhoff DJ, Lenkinski RE, Gonzalez RG, Navia BA (2003). A multi-center 1H MRS study of the AIDS dementia complex: validation and preliminary analysis. *J Magn Reson Imaging* **17**: 625–633.
- Lipton SA (1993). Human immunodeficiency virus-infected macrophages, gp120, and N-methyl-D-aspartate receptor mediated neurotoxicity. *Ann Neurol* **33**: 227–228.
- Mankowski JL, Queen SE, Tarwater PJ, Adams RJ, Guilarte TR (2003). Elevated peripheral benzodiazepine receptor expression in simian immunodeficiency virus encephalitis. *J NeuroVirol* **9**: 94–100.
- McArthur JC, Haughey N, Gartner S, Conant K, Pardo C, Nath A, Sacktor N (2003). Human immunodeficiency virus-associated dementia: an evolving disease. *J NeuroVirol* **9**: 205–221.
- Myers R, Manjil LG, Cullen BM, Price GW, Frackowiak RS, Cremer JE (1991). Macrophage and astrocyte populations in relation to [³H]PK 11195 binding in rat cerebral cortex following a local ischaemic lesion. *J Cereb Blood Flow Metab* **11**: 314–322.
- Neuen-Jacob E, Arendt G, Wendtland B, Jacob B, Schneeweis M, Wechsler W (1993). Frequency and topographical distribution of CD68-positive macrophages and HIV-1 core proteins in HIV-associated brain lesions. *Clin Neuropathol* **12**: 315–324.
- Nicolini A, Ajmone-Cat MA, Bernardo A, Levi G, Minghetti L (2001). Human immunodeficiency virus type-1 Tat protein induces nuclear factor (NF)-kappaB activation and oxidative stress in microglial cultures by independent mechanisms. *J Neurochem* **79**: 713–716.
- Pappata S, Lévassieur M, Gunn RN, Myers R, Crouzel C, Syrota A, Jones T, Kreutzberg GW, Banati RB (2000). Thalamic microglial activation in ischemic stroke detected in vivo by PET and [¹¹C]PK11195. *Neurology* **55**: 1052–1054.
- Price GW, Ahier RG, Hume SP, Myers R, Manjil L, Cremer JE, Luthra SK, Pascali C, Pike V, Frackowiak RS (1990). In vivo binding to peripheral benzodiazepine binding sites in lesioned rat brain: comparison between [³H]PK11195 and [¹⁸F]PK14105 as markers for neuronal damage. *J Neurochem* **55**: 175–185.
- Pulliam L, Gascon R, Stubblebine M, McGuire D, McGrath MS (1997). Unique monocyte subset in patients with AIDS dementia. *Lancet* **349**: 692–695.
- Robb RA (2001). The biomedical imaging resource at Mayo Clinic. *IEEE Trans Med Imaging* **20**: 854–867.
- Rottman JB, Ganley KP, Williams K, Wu L, Mackay CR, Ringler DJ (1997). Cellular localization of the chemokine receptor CCR5. Correlation to cellular targets of HIV-1 infection. *Am J Pathol* **151**: 1341–1351.
- Sauvageau A, Desjardins P, Lozeva V, Rose C, Hazell AS, Bouthillier A, Butterworth RF (2002). Increased expression of “peripheral-type” benzodiazepine receptors in human temporal lobe epilepsy: implications for PET imaging of hippocampal sclerosis. *Metab Brain Dis* **17**: 3–11.
- Stephenson DT, Schober DA, Smalstig EB, Mincy RE, Gehlert DR, Clemens JA (1995). Peripheral benzodiazepine receptors are colocalized with activated microglia following transient global forebrain ischemia in the rat. *J Neurosci* **15**: 5263–5274.
- Takahashi K, Wesselingh SL, Griffin DE, McArthur JC, Johnson RT, Glass JD (1996). Localization of HIV-1 in human brain using polymerase chain reaction/in situ hybridization and immunocytochemistry. *Ann Neurol* **39**: 705–711.
- Turner MR, Cagnin A, Turkheimer FE, Miller CC, Shaw CE, Brooks DJ, Leigh PN, Banati RB (2004). Evidence of widespread cerebral microglial activation in amyotrophic lateral sclerosis: an [¹¹C](R)-PK11195 positron emission tomography study. *Neurobiol Dis* **15**: 601–609.
- Vallat AV, De Girolami U, He J, Mhashilkar A, Marasco W, Shi B, Gray F, Bell J, Keohane C, Smith TW, Gabuzda D (1998). Localization of HIV-1 co-receptors CC-R5 and CXCR4 in the brain of children with AIDS. *Am J Pathol* **152**: 167–178.
- Venneti S, Lopresti BJ, Wang G, Bissel SJ, Mathis CA, Meltzer CC, Boada F, Capuano S, 3rd, Kress GJ, Davis DK, Ruszkiewicz J, Reynolds IJ, Murphey-Corb M, Trichel AM, Wisniewski SR, Wiley CA (2004). PET imaging of brain macrophages using the peripheral benzodiazepine receptor in a macaque model of neuroAIDS. *J Clin Invest* **113**: 981–989.
- von Giesen HJ, Wittsack HJ, Wenserski F, Koller H, Hefter H, Arendt G (2001). Basal ganglia metabolite abnormalities in minor motor disorders associated with human immunodeficiency virus type 1. *Arch Neurol* **58**: 1281–1286.
- Vowinckel E, Reutens D, Becher B, Verge G, Evans A, Owens T, Antel JP (1997). PK11195 binding to the peripheral benzodiazepine receptor as a marker of microglia activation in multiple sclerosis and experimental autoimmune encephalomyelitis. *J Neurosci Res* **50**: 345–353.
- Ward JM, O’Leary TJ, Baskin GB, Benveniste R, Harris CA, Nara PL, Rhodes RH (1987). Immunohistochemical localization of human and simian immunodeficiency viral

- antigens in fixed tissue sections. *Am J Pathol* **127**: 199–205.
- Wesselingh SL, Takahashi K, Glass JD, McArthur JC, Griffin JW, Griffin DE (1997). Cellular localization of tumor necrosis factor mRNA in neurological tissue from HIV-infected patients by combined reverse transcriptase/polymerase chain reaction in situ hybridization and immunohistochemistry. *J Neuroimmunol* **74**: 1–8.
- Yeh MW, Kaul M, Zheng J, Nottet HS, Thylin M, Gendelman HE, Lipton SA (2000). Cytokine-stimulated, but not HIV-infected, human monocyte-derived macrophages produce neurotoxic levels of l-cysteine. *J Immunol* **164**: 4265–4270.